Application of the "Full Cavitation Model" to the fundamental study of cavitation in liquid metal processing

G S B Lebon[1], K Pericleous[1], I Tzanakis[2] and D Eskin[2]

[1] Centre for Numerical Modelling and Process Analysis, The University of Greenwich, London SE10 9LS, United Kingdom
[2] Brunel Centre for Advanced Solidification Technology (BCAST), Brunel University, Uxbridge, Middlesex UB8 3PH, United Kingdom

Email: G.S.B.Lebon@greenwich.ac.uk

Abstract. Ultrasonic cavitation treatment of melt significantly improves the downstream properties and quality of conventional and advanced metallic materials. However, the transfer of this technology has been hindered by difficulties in treating large volumes of liquid metal. To improve the understanding of cavitation processing efficiency, the Full Cavitation Model, which is derived from a reduced form of the Rayleigh-Plesset equation, is modified and applied to the two-phase problem of bubble propagation in liquid melt. Numerical simulations of the sound propagation are performed in the microsecond time scale to predict the maximum and minimum acoustic pressure amplitude fields in the domain. This field is applied to the source term of the bubble transport equation to predict the generation and destruction of cavitation bubbles in a time scale relevant to the fluid flow. The use of baffles to limit flow speed in a launder conduit is studied numerically, to determine the optimum configuration that maximizes the residence time of the liquid in high cavitation activity regions. With this configuration, it is then possible to convert the batch processing of liquid metal into a continuous process. The numerical simulations will be validated against water and aluminium alloy experiments, carried out at Brunel University.

1. Introduction

Significant improvement of quality and properties in metallic materials is observed when melt is treated with ultrasound [1][2]. These improvements are primarily due to ultrasonic cavitation, with the creation, growth, pulsation, and collapse of bubbles in the liquid. However, this technology has not been successfully transferred to the industry due to the difficulty in treating large volumes of liquid metal, as is required by processes such as continuous casting. A fundamental study of the ultrasonic treatment of melt is thus required to circumvent these difficulties.

The full cavitation model was developed by Athavale et al [3][4] to provide the capability for multidimensional simulation of cavitating flows, the modelling of which is crucial to the design of many engineering devices [5]. In their approach, the authors derived source terms for the bubble mass fraction transport equation from the Rayleigh-Plesset equation [6], which governs the evolution of a spherical bubble [7], to predict the formation and collapse of bubbles in cavitating flows. This model has been used in the modelling of the solidification structure evolution by Nastac [8].

In this study, the full cavitation model is modified to compute the bubble concentration in a launder. The novelty here is to understand the effect of ultrasonic treatment on flowing melt, paving the way to the ultrasonic treatment of liquid metal in batch.

2. Numerical method

The approach consists of solving the wave equation and using the acoustic pressure solution in the source term of a non-condensable gas mass fraction, f_g, equation. The Reynolds-Averaged Navier-Stokes (RANS) equations are solved along with the mass fraction transport equation. The density of the fluid is calculated as a function of the non-condensable gas mass fraction.

2.1. Governing equations

2.1.1. Fluid equations. Fluid flow is governed by the RANS equations:

$$\frac{\partial \rho}{\partial t} + \nabla \cdot (\rho \boldsymbol{u}) = 0$$
$$\frac{\partial (\rho u_i)}{\partial t} + \nabla \cdot (\rho \boldsymbol{u} u_i) = \nabla \cdot [(\mu + \mu_t) \nabla u_i] + S_{u_i} \quad (2)$$

where ρ is the fluid density, $\boldsymbol{u}$ is the fluid velocity, μ is the dynamic viscosity, μ_t is the eddy viscosity, and S_{u_i} are the momentum sources. The fluid density is related to the vapour and non-condensable gas mass fractions, f_v and f_g, according to:

$$\frac{1}{\rho} = \frac{f_v}{\rho_v} + \frac{f_g}{\rho_g} + \frac{1 - f_v - f_g}{\rho_l} \quad (3)$$

where ρ_v is the density of the vapour in the bubbles, ρ_g is the density of the non-condensable gas–hydrogen for aluminium melt–, and ρ_l is the liquid density [4]. The standard $k - \varepsilon$ model [9] is used for closure in the RANS formulation.

2.1.2. Wave equation. The wave equation is:

$$\frac{\partial^2 p}{\partial t^2} - c^2 \frac{\partial}{\partial x_i}\left(\frac{\partial p}{\partial x_i}\right) = c^2 S_p \quad (4)$$

where p is acoustic pressure, c is the speed of sound, and S_p are the wave source terms.

2.1.3. Full cavitation model. The liquid-bubble mass transfer is governed by the cavity transport equation [4]:

$$\frac{\partial (\rho_v f_v)}{\partial t} + \nabla \cdot (\rho_v \boldsymbol{u} f_v) = \nabla \cdot (\Gamma \nabla f_v) + S_G - S_C \quad (5)$$

where $\Gamma = \mu + \mu_t$ is the effective exchange coefficient, and S_G and S_C are the mass transfer source terms related to the growth and collapse of the cavitation bubbles respectively. S_G and S_C are derived from the Rayleigh-Plesset equation [6] and are given by [4]:
when $p < p_v$:

$$S_G = C_G \frac{\sqrt{k}}{S} \rho_l \rho_v \left[\frac{2}{3}\frac{p_v - p}{\rho_l}\right]^{\frac{1}{2}} \left(1 - f_v - f_g\right) \quad (6)$$

when $p > p_v$:

$$S_C = C_c \frac{\sqrt{k}}{S} \rho_l \rho_v \left[\frac{2}{3}\frac{p - p_v}{\rho_l}\right]^{\frac{1}{2}} (f_v) \quad (7)$$

where $C_G = 0.02$ and $C_C = 0.01$. p_v is the sum of the vapor pressure and an estimation of the local values of turbulent pressure fluctuations [4]:

$$p_v = p_{sat} + 0.39 \rho k / 2 \quad (8)$$

2.1.4. Modification of the full cavitation model for melt modelling. In liquid aluminium, cavitation due to vapour pressure is hard to attain and cavitation is mainly due to non-condensable gases, mainly hydrogen. The full cavitation model is therefore modified to account for this difference.

The vapour mass fraction is ignored and the density and mass fraction transport equations are re-written as:

$$\frac{1}{\rho} = \frac{f_g}{\rho_g} + \frac{1-f_g}{\rho_l} \tag{9}$$

$$\frac{\partial(\rho_g f_g)}{\partial t} + \nabla \cdot \left(\rho_g \boldsymbol{u} f_g\right) = \nabla \cdot \left(\Gamma \nabla f_g\right) + S_G - S_C \tag{10}$$

where the sources are now given by:
when $p_{min} < (p_g + 0.39\rho k/2)$:

$$S_G = C_G \frac{\sqrt{v_{ch}}}{s} \rho_l \rho_g \left[\frac{2}{3}\frac{p_g + 0.39\rho k/2 - p}{\rho_l}\right]^{\frac{1}{2}} \left(1 - f_g\right) \tag{11}$$

when $p_{max} > (p_g + 0.39\rho k/2)$:

$$S_C = C_c \frac{\sqrt{v_{ch}}}{s} \rho_l \rho_g \left[\frac{2}{3}\frac{p - p_g - 0.39\rho k/2}{\rho_l}\right]^{\frac{1}{2}} \left(f_g\right) \tag{12}$$

The coefficients of Athavale et al [3] are used in the source terms, although their application to this modified model has to be validated from experiment. v_{ch} is estimated as 1 % of the mean flow speed.

2.1.5. Modelling flow and bubble generation in the macro- time scale. In order to run simulations in a time scale more appropriate for the flow, the minimum and maximum acoustic pressures p_{min} and p_{max} are first computed from a microsecond time scale simulation, with the time-step chosen so as to ensure that a minimum of 20 points are available per ultrasonic cycle. These stored pressures are then respectively applied to the generation and collapse source terms given by equations (11) and (12).

2.2. Discretization

2.2.1. Leap-frog scheme for the wave equation. Wave equation (4) is discretized using a second-order scheme. Acoustic pressures are stored at cell centres at each time step. Velocity components are stored on faces half time step apart from the pressures.

$$p^{\mathrm{k}} = p^{k-1} - \frac{c\Delta t}{x_i}\left(u_{i,dwnd}^{k-\frac{1}{2}} - u_{i,upwnd}^{k-\frac{1}{2}}\right) + S\Delta t$$

$$u_i^{k+\frac{1}{2}} = u_i^{k-\frac{1}{2}} - c\Delta t\left(p_{dwnd}^{k} - p_{upwnd}^{k}\right) + S_i\Delta t$$

where u_i are the wave velocities.

2.2.2. Finite volume method. The finite volume method is used to discretize the RANS and transport equations.

3. Problem description

In order to model continuous treatment of melt, the launder, shown in Figure 1, is used for the computational domain. The sonotrode is at the center of the domain and the tip is immersed 1 cm below the liquid surface. The inlet and outlet are at the lowest and highest y values respectively. Clean liquid, that is without bubble, enters the domain at a velocity of 0.01 m s^{-1} in the y direction. The launder problem is solved for both water and aluminium. The launder boundaries are full reflective to ultrasound.

The distance between the baffles is varied as a function of the sound wavelength. In water, the wavelength λ of ultrasound at 20 kHz is 7.4 cm, and in aluminium, the wavelength is 23 cm. The case is run for each liquid for the following distances L between baffles: 0.5 λ, 1 λ, and 1.5 λ. The material properties for the melt – aluminium –, and water are shown in Table 1.

Table 1. Material properties of liquid aluminium and water [1].

Material Property	Aluminium (700 ºC)	Water (20 ºC)
Sound speed $\boldsymbol{c}$ (m s^{-1})	4600	1481
Density $\boldsymbol{\rho_l}$ (kg m^{-3})	2350	1000
Dynamic viscosity $\boldsymbol{\mu}$ (mPa s)	1.3	0.798
Surface tension (hydrogen interface) $\boldsymbol{S}$ (N m^{-1})	0.87	0.072
Vapour pressure $\boldsymbol{p_{sat}}$ (kPa)	0	4.24

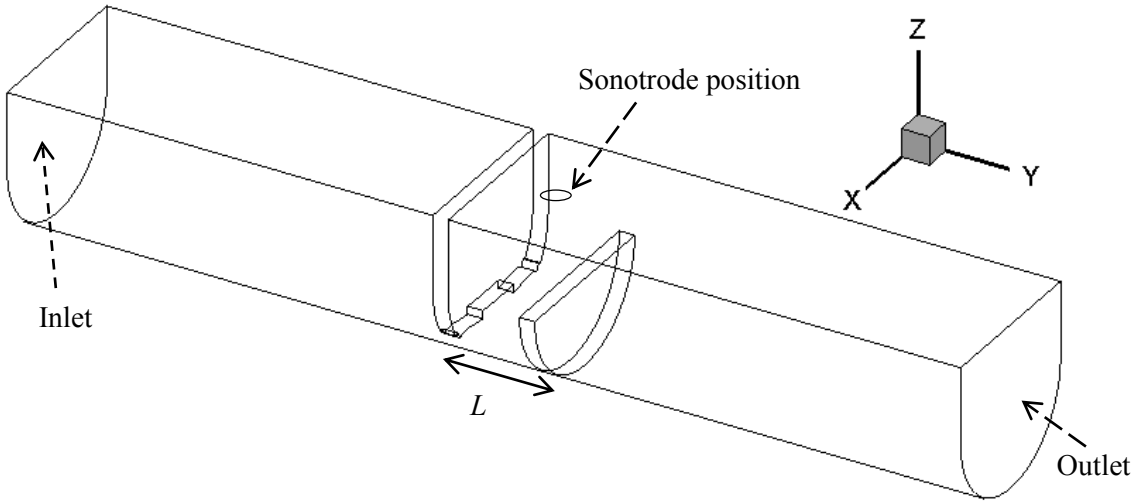

Figure 1. 50 cm x 9 cm x 8 cm launder. L denotes the length between baffles, of thickness 8 mm each. The sonotrode is immersed 1 cm into the free surface at the center of the domain.

4. Results

4.1. Acoustic run

The wave equation (4) is solved with a time step of 1 μs, and the minimum and acoustic pressure in the domain is obtained, as shown in Figure 2 and Figure 3 for the baffles separated at 37 cm, half the wavelength of sound in water at 20 ºC. As expected, the extreme values of pressure are at their highest just below the sonotrode, in the middle of the domain. The cavitation threshold of -1.0 x 10^5 Pa is achieved in the whole domain for this configuration.

Figure 2. Predicted minimum acoustic pressure (Pa) in domain for a configuration with baffles separated at a distance of 0.5 $\boldsymbol{\lambda}$ for water.

Figure 3. Predicted maximum acoustic pressure (Pa) in domain for a configuration with baffles separated at a distance of 0.5 $\boldsymbol{\lambda}$ for water.

The low values of maximum acoustic pressure at the left of the first (upstream) separation hinders the collapse of bubbles, and can yield large values of bubble concentration upstream, as shown in the next section.

4.2. Cavitation run

The full cavitation model is run for 20 s of simulation time with a time step of 1 ms for both water and aluminium. Figure 4 and Figure 5 show the bubble mass fraction below the sonotrode at the end of the run time for both the water and aluminium simulations. Figure 6 and Figure 7 describe the variation of the bubble concentration along the axis of the launder.

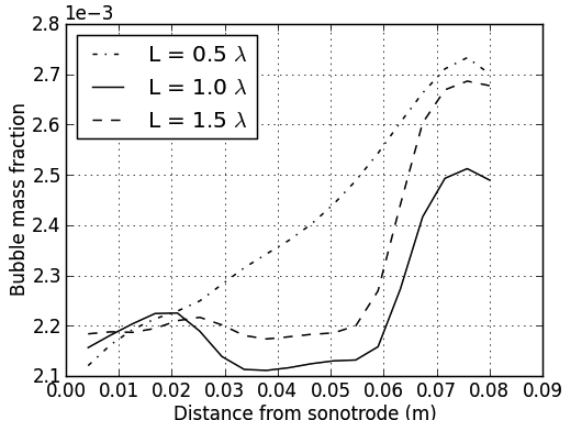

Figure 4. Bubble mass fraction along the axis of the sonotrode for water after a run time of 20 s. Mass fraction values are taken along the axis of the sonotrode.

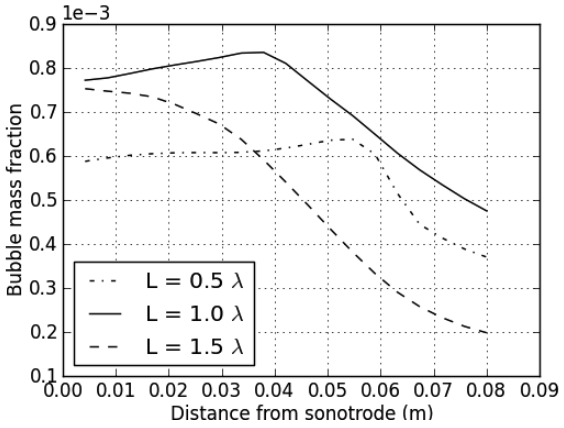

Figure 5. Bubble mass fraction along the axis of the sonotrode for aluminium after a run time of 20 s. Mass fraction values are taken along the axis of the sonotrode.

For water, the baffle configuration that maximises the bubble concentration in the domain is when the baffles are separated by a distance of 0.5 λ. The flow pattern generated with this optimum separation distance effectively convects the bubbles downstream, resulting in a large the bubble concentration downstream. For aluminium, a separation of 1.0 λ between the baffles is the optimum configuration. More bubbles are also convected downstream with this configuration.

The small opening of the upstream baffles forces a strong current at the bottom of the launder, resulting in a recirculation of the fluid beneath the sonotrode region, as shown in Figure 8 for aluminium and a baffle separation of 1.0 λ. The shortest path for exiting the domain is along the strong bottom current. Table 2 lists the shortest residence time for each configuration.

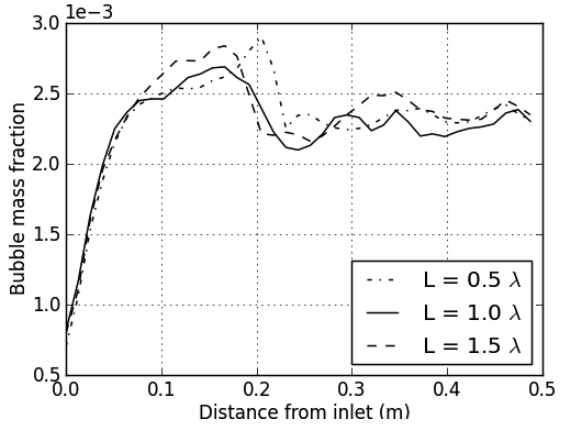

Figure 6. Bubble mass fraction across the launder for water after a run time of 20 s. Mass fraction values are taken along the axis of the launder.

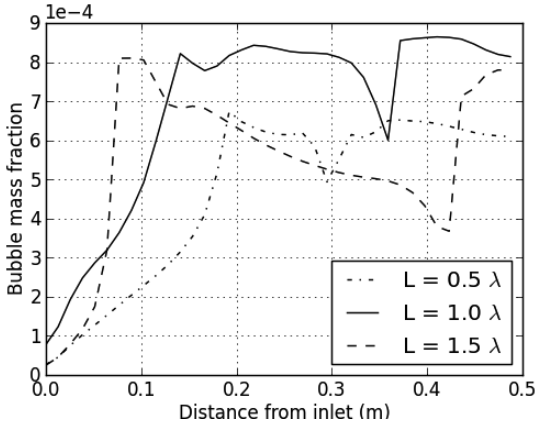

Figure 7. Bubble mass fraction across the launder for aluminium after a run time of 20 s. Mass fraction values are taken along the axis of the launder.

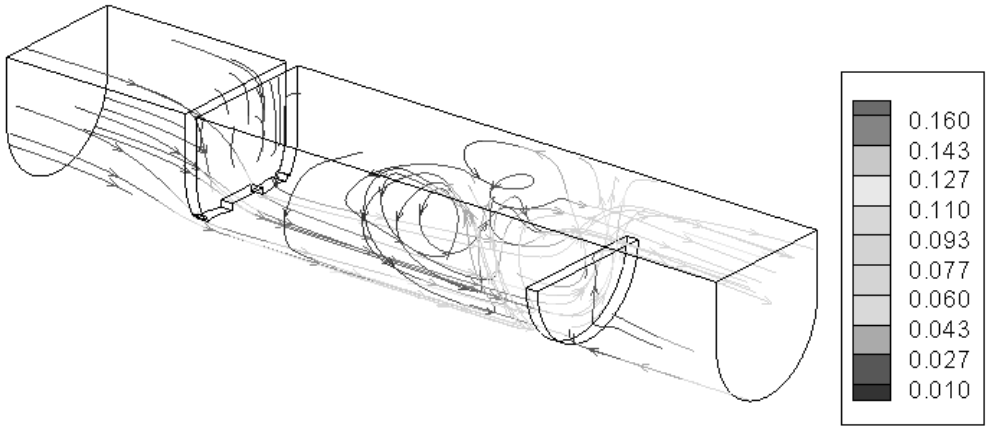

Figure 8. Recirculation in configuration with baffles separated at a distance of 1.0 $\boldsymbol{\lambda}$ for aluminium. Contour colours represent speed in m s^{-1}.

Table 2. Minimum residence time (s) for each configuration. The following values denotes the time taken for the liquid to leave the domain along the shortest path.

L (λ)	$\boldsymbol{L}_{\text{aluminium}}$ (cm)	Aluminium at 700 ºC (s)	$\boldsymbol{L}_{\text{water}}$ (cm)	Water at 20 ºC (s)
0.5	11.5	16.0	3.7	21.2
1.0	23.0	12.5	7.4	15.5
1.5	34.5	9.8	11.1	13.8

5. Conclusion

In search of a complete model, multi-scale model for the ultrasonic treatment of liquid metals, this study computes the bubble concentration for the flow in a launder with baffles to create recirculations around the sonotrode. Cavitation threshold pressures are achieved in the large part of the domain, and bubble concentration as a function of baffle separation can be predicted in a timescale of seconds. The optimum configuration for the ultrasonic treatment of aluminium melt is found to be with a baffle separation of 1.0 λ.

Acknowledgement
The authors are grateful to the UK Engineering and Physical Sciences Research Council (EPSRC) for financial assistance for this research in contract numbers: EP/K00588X/1 and EP/K005804/1.

References
[1] Eskin G 1998 *Ultrasonic Treatment of Light Alloy Melts* (Amsterdam: Gordon and Breach)
[2] Campbell J 1981 *Int. Met. Rev.* **26** 71
[3] Athavale M, Jiang Y, Li H and Singhal A 2002 *Int. J. Rot. Mach.* **8** 45
[4] Singhal A, Athavale M, Li H and Jiang Y 2002 *J. Fluid Eng.* **124** 617
[5] Dular M, Bachert R, Stoffel B, and Širok B 2005 *Eur. J. Mech B.Fluid* **24** 522
[6] Plesset MS 1949 *J. Appl. Mech.* **16** 227
[7] Brennen C 1995 *Cavitation and Bubble Dynamics* (Oxford: Oxford University Press)
[8] Nastac L 2011 *Metall. Mater. Trans. B* **42** 1297
[9] Launder B and Spalding D 1974 *Comp. Meth. In Appl. Mech. & Eng.* **3** 269